Documentation of the gyrokinetic database GKDB

Y. Camenen and the GKDB team

Last update: November 5, 2018

Contents

Chapter 1

Preamble

The gyrokinetic database (GKDB) stores results from linear and non-linear δf, flux-tube gyrokinetic simulations. The present document summarises the names, conventions and normalisations adopted for the inputs and outputs of the GKDB.

The normalised inputs and outputs are independent of ρ_* consistently with the local approximation and a spectral representation is assumed in the perpendicular plane (i.e. homogeneous turbulence).

S.I. units are used everywhere with the exception of temperatures given in eV. This means that kT is noted T as is customary in plasma physics.

Chapter 2

Database structure

ids_properties_tag

ids_properties_id	integer
tag_id	integer

tag

name	text
comment	text

ids_properties

provider	text
creation_date	timestamp
comment	text

code

ids_properties_id	integer
name	text
version	text
parameters	jsonb

species_all

ids_properties_id	integer
beta_reference	real
debye_length_reference	real
velocity_tor_norm	real
shearing_rate_norm (NL)	real
zeff	real

model

ids_properties_id	integer
initial_value_run (1 if NL)	boolean
non_linear_run	boolean
time_interval_norm (NL)	array 2×1
include_a_field_parallel	boolean
include_b_field_parallel	boolean
inconsistent_curvature_drift	boolean
include_centrifugal_effects	boolean
collisions_pitch_only	boolean
collisions_momentum_conservation	boolean
collisions_energy_conservation	boolean
collisions_finite_larmor_radius	boolean

flux surface

ids_properties_id	integer
r_minor_norm	real
q	real
magnetic_shear_r_minor	real
pressure_gradient_norm	real
ip_sign	smallint
b_field_tor_sign	smallint
shape_coefficients_c	array $(N_{sh}+1) \times 1$
shape_coefficients_c	array $N_{sh} \times 1$
dc_dr_minor_norm	array $(N_{sh}+1) \times 1$
dc_dr_minor_norm	array $N_{sh} \times 1$
elongation	real
triangularity_upper	real
triangularity_lower	real

wavevector

ids_properties_id	integer
radial_component_norm	real
binormal_component_norm	real
poloidal_turns (1 if NL)	integer

collisions

species1_id	integer
species2_id	integer
collisionality_norm	real

species

ids_properties_id	integer
charge_norm	real
mass_norm	real
density_norm	real
temperature_norm	real
density_log_gradient_norm	real
temperature_log_gradient_norm	real
velocity_toroidal_gradient_norm	real

eigenmode

wavevector_id	integer
growth_rate_norm (L)	real
frequency_norm (L)	real
growth_rate_tolerance (L)	real
phi_potential_perturbed_norm_real	array $N_\theta \times 1$
phi_potential_perturbed_norm_imaginary	array $N_\theta \times 1$
a_field_parallel_perturbed_norm_real	array $N_\theta \times 1$
a_field_parallel_perturbed_norm_imaginary	array $N_\theta \times 1$
b_field_parallel_perturbed_norm_real	array $N_\theta \times 1$
b_field_parallel_perturbed_norm_imaginary	array $N_\theta \times 1$
poloidal_angle	array $N_\theta \times 1$
phi_potential_perturbed_weight	real
phi_potential_perturbed_parity	real
a_field_parallel_perturbed_weight	real
a_field_parallel_perturbed_parity	real
b_field_parallel_perturbed_weight	real
b_field_parallel_perturbed_parity	real

fluxes_norm

species_id	integer
eigenmode_id	integer
particles_phi_potential	real
particles_a_field_parallel	real
particles_b_field_parallel	real
momentum_tor_parallel_phi_potential	real
momentum_tor_parallel_a_field_parallel	real
momentum_tor_parallel_b_field_parallel	real
momentum_tor_perpendicular_phi_potential	real
momentum_tor_perpendicular_a_field_parallel	real
momentum_tor_perpendicular_b_field_parallel	real
energy_phi_potential	real
energy_a_field_parallel	real
energy_b_field_parallel	real

moments_norm_rotating_frame

species_id	integer
eigenmode_id	integer
density_real	array $N_\theta \times 1$
density_imaginary	array $N_\theta \times 1$
velocity_parallel_real	array $N_\theta \times 1$
velocity_parallel_imaginary	array $N_\theta \times 1$
temperature_parallel_real	array $N_\theta \times 1$
temperature_parallel_imaginary	array $N_\theta \times 1$
temperature_perpendicular_real	array $N_\theta \times 1$
temperature_perpendicular_imaginary	array $N_\theta \times 1$
density_gyroaveraged_real	array $N_\theta \times 1$
density_gyroaveraged_imaginary	array $N_\theta \times 1$
velocity_parallel_gyroaveraged_real	array $N_\theta \times 1$
velocity_parallel_gyroaveraged_imaginary	array $N_\theta \times 1$
temperature_parallel_gyroaveraged_real	array $N_\theta \times 1$
temperature_parallel_gyroaveraged_imaginary	array $N_\theta \times 1$
temperature_perpendicular_gyroaveraged_real	array $N_\theta \times 1$
temperature_perpendicular_gyroaveraged_imaginary	array $N_\theta \times 1$

fluxes_integrated_norm (NL)

species_id	integer
ids_properties_id	integer
particles_phi_potential	real
particles_a_field_parallel	real
particles_b_field_parallel	real
momentum_tor_parallel_phi_potential	real
momentum_tor_parallel_a_field_parallel	real
momentum_tor_parallel_b_field_parallel	real
momentum_tor_perpendicular_phi_potential	real
momentum_tor_perpendicular_a_field_parallel	real
momentum_tor_perpendicular_b_field_parallel	real
energy_phi_potential	real
energy_a_field_parallel	real
energy_b_field_parallel	real

Chapter 3

Conventions and normalisations

3.1 Cylindrical and flux coordinate systems

The ITER coordinate convention is adopted for the GKDB. The corresponding index in the COordinate COnventionS system [1] is COCOS=11.

3.1.1 Cylindrical coordinate system (R, φ, Z)

A right-handed cylindrical coordinate system (R, φ, Z), with R the major radius, Z the elevation and φ the toroidal angle (increasing when anticlockwise from above) is used to describe the flux surfaces, see Fig. 3.1.

The magnetic equilibrium is assumed to be axisymmetric and the poloidal contours of the flux surface $\Psi(R, Z) = \Psi_0$, with Ψ the poloidal magnetic flux, are noted $\{R_{\Psi_0}, Z_{\Psi_0}\}$. For COCOS=11, Ψ is minimum at the magnetic axis for a plasma current flowing in the direction of $\nabla\varphi$ and maximum at the magnetic axis for a plasma current flowing in the direction opposite to $\nabla\varphi$.
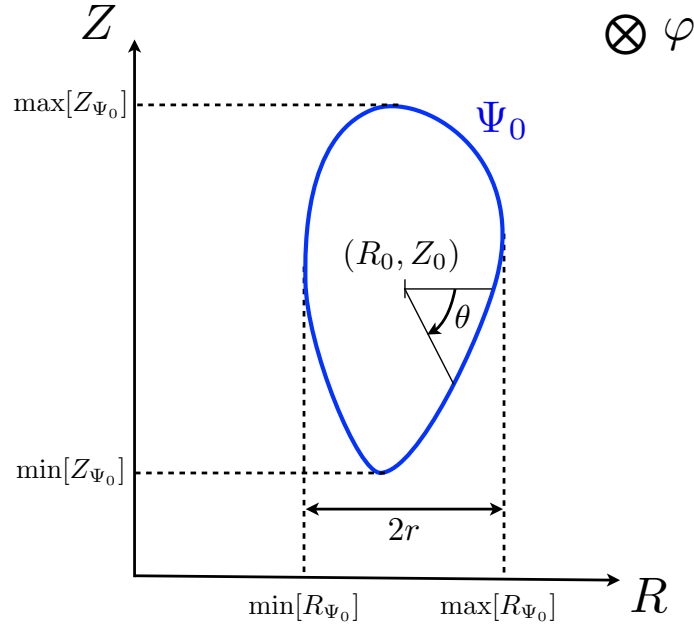
Figure 3.1: Coordinate conventions used in the GKDB (COCOS=11, [1]).

3.1.2 Flux coordinate system (r, θ, φ)

A right handed flux coordinate system (r, θ, φ) is now introduced.

Flux surface center

To start with, a reference point (R_0, Z_0) is defined for the flux surface of interest $\{R_{\Psi_0}, Z_{\Psi_0}\}$:

$$R_0 = \frac{1}{2}\left[\max[R_{\Psi_0}] + \min[R_{\Psi_0}]\right] \tag{3.1}$$

$$Z_0 = \frac{1}{2}\left[\max[Z_{\Psi_0}] + \min[Z_{\Psi_0}]\right] \tag{3.2}$$

The reference point (R_0, Z_0) will be used in the following to define the poloidal angle. Note that (R_0, Z_0) is not the position of the magnetic axis, although it can be in some particular cases.

Radial coordinate

The radial coordinate r is defined as

$$r = \frac{1}{2}\left[\max[R_{\Psi_0}] - \min[R_{\Psi_0}]\right] \tag{3.3}$$

It has the dimension of a length and is constant on a flux surface, by definition. The radial coordinate of the flux surface $\Psi = \Psi_0$ is noted r_0.

Poloidal angle

The poloidal angle is defined from the following relationships:

$$\cos\theta = \frac{R_{\Psi_0} - R_0}{[(R_{\Psi_0} - R_0)^2 + (Z_{\Psi_0} - Z_0)^2]^{1/2}} \tag{3.4}$$

$$\sin\theta = -\frac{Z_{\Psi_0} - Z_0}{[(R_{\Psi_0} - R_0)^2 + (Z_{\Psi_0} - Z_0)^2]^{1/2}} \tag{3.5}$$

The poloidal angle is zero at the low field side midplane (the midplane is defined with respect to the flux surface $\Psi = \Psi_0$ and corresponds to $Z = Z_0$) and increases clockwise when the tokamak vertical axis is on the left of the flux surface, see Fig. 3.1.

3.2 Flux surface average

In a few cases, flux surface averaged quantities will be required. We adopt here the flux surface average definition that arises when taking the integral of a conservation equation over the volume enclosed by a flux surface (i.e. the standard procedure to built 1D transport equations in tokamaks, see for instance [2]).

The flux surface average of a quantity A is then given by

$$< A >= \frac{\int A(\mathbf{x})\delta(r - r_0)\,\mathrm{d}^3 x}{\int \delta(r - r_0)\,\mathrm{d}^3 x} \tag{3.6}$$

where r_0 is the radial coordinate of the flux surface on which the average is being performed, r is the value of the radial coordinate at position $\mathbf{x}$, δ is the Dirac function and the integral is being performed over the whole plasma volume (or entire world, it does not matter).

Noting that the surface element $\mathrm{d}S$ on a flux surface is related to the volume element $\mathrm{d}^3 x$ by

$$\mathrm{d}^3 x = \mathrm{d}S\frac{\mathrm{d}r}{|\nabla r|} \tag{3.7}$$

with r an arbitrary flux surface label (taken here to be the radial coordinate defined above), a convenient alternative (and equivalent) expression for the flux surface average is obtained:

$$< A >= \frac{1}{V'} \oint A \frac{\mathrm{d}S}{|\nabla r|} \tag{3.8}$$

with $V' = \frac{\partial V}{\partial r}$ and V being the volume enclosed by the flux surface labelled by r.

3.3 Normalisations

All quantities in the database (inputs and outputs) are normalised using six reference quantities. These reference quantities (fundamental reference quantities) are listed below and then used to built other convenient normalising factors (derived reference quantities).

In principle, reference quantities do not need to be specified, as the purpose of the database is to relate normalised inputs to normalised outputs. However, if the choice of reference quantities is left arbitrary, the same physical inputs could lead to different normalised inputs in the database depending on the normalisation choice. This is not desirable and the reference quantities are therefore imposed.

3.3.1 Fundamental reference quantities

The six fundamental reference quantities are:

- $q_{\mathrm{ref}} = e = 1.602176634 \times 10^{-19} \, \mathrm{C}$, the positive elementary charge

- $m_{\mathrm{ref}} = m_D = 3.343583719 \times 10^{-27} \, \mathrm{kg}$, the Deuterium mass

- $T_{\mathrm{ref}} = T_e(r_0, \theta = 0)$, the electron temperature at $\theta = 0$

- $n_{\mathrm{ref}} = n_e(r_0, \theta = 0)$, the electron density at $\theta = 0$

- $L_{\mathrm{ref}} = R_0$, the reference length

- $B_{\mathrm{ref}} = B_t(R_0, Z_0)$, the reference magnetic field (toroidal magnetic field at the flux surface center)

3.3.2 Derived reference quantities

For convenience, the following reference quantities are defined:

- $v_{\mathrm{thref}} = \sqrt{\frac{2T_{\mathrm{ref}}}{m_{\mathrm{ref}}}}$, the reference thermal velocity

- $\rho_{\mathrm{ref}} = \frac{m_{\mathrm{ref}} v_{\mathrm{thref}}}{q_{\mathrm{ref}} B_{\mathrm{ref}}}$, the reference Larmor radius

Chapter 4

Inputs

4.1 Species

For each species s, the background distribution function is supposed to be a local Maxwellian. Poloidal asymmetry in the background induced by centrifugal effects is allowed. Poloidally asymmetric quantities are given in input at $\theta = 0$. Poloidal asymmetry induced by anisotropic temperatures is not included yet, but could be introduced if need be.

At this stage, the database only stores runs with kinetic electron species (adiabatic electrons not allowed). An arbitrary number of kinetic species is allowed, including several instance of the same species, but quasineutrality has to be ensured.

4.1.1 Charge

$$\texttt{charge\_norm} = Z_{sN} = \frac{q_s}{q_{\mathrm{ref}}}$$

4.1.2 Mass

$$\texttt{mass\_norm} = m_{sN} = \frac{m_s}{m_{\mathrm{ref}}}$$

4.1.3 Density

$$\texttt{density\_norm} = n_{sN} = \frac{n_s}{n_{\mathrm{ref}}}$$

4.1.4 Logarithmic density gradient

$$\texttt{density\_log\_gradient\_norm} = L_{\mathrm{ref}}/L_{n_s} = -L_{\mathrm{ref}}\frac{1}{n_s}\frac{\partial n_s}{\partial r}$$

Positive for peaked profiles.

4.1.5 Temperature

$$\texttt{temperature\_norm} = T_{sN} = \frac{T_s}{T_{\mathrm{ref}}}$$

4.1.6 Logarithmic temperature gradient

$$\texttt{temperature\_log\_gradient\_norm} = L_{\mathrm{ref}}/L_{T_s} = -L_{\mathrm{ref}}\frac{1}{T_s}\frac{\partial T_s}{\partial r}$$

Positive for peaked profiles.

4.1.7 Toroidal velocity

$$\texttt{velocity\_tor\_norm} = u_N = \frac{L_{\text{ref}}}{v_{\text{thref}}}\omega_\Phi$$

Positive for a flow in the direction of $\nabla\varphi$.

All species are assumed to have a purely toroidal flow $\mathbf{v}_s = R^2\omega_\Phi\nabla\varphi$ with a common toroidal angular frequency proportional to the background electric field:

$$\omega_\Phi = -2\pi\frac{\partial\Phi}{\partial\Psi},$$

with Φ the background electrostatic potential. This assumption is consistent with the ordering used in local gyrokinetic codes, as ω_Φ is the lowest order flow in a ρ_* expansion according to neoclassical theory [3].

4.1.8 Perpendicular flow shear (non-linear runs only)

The $E \times B$ shearing rate is given by:

$$\texttt{shearing\_rate\_norm} = \gamma_{E_N} = -\frac{L_{\text{ref}}}{v_{\text{thref}}}\frac{1}{B_{\text{ref}}}\left(\frac{\partial\Psi}{\partial r}\right)^2\frac{\partial^2\Phi}{\partial\Psi^2}$$

This input is only used in the database for non-linear runs (for linear runs, only $\gamma_{E_N} = 0$ is allowed).

4.1.9 Parallel flow shear

The parallel flow shear is assumed to arise entirely from the shear in a toroidal flow of constant angular frequency on a flux surface. The possibility to have a species dependent toroidal velocity gradient with $\omega_{\varphi,s} \neq \omega_\Phi$ is retained. Strictly speaking, this is inconsistent with the local limit assumption $\rho_* \to 0$ but can be interesting for the interpretation of tokamak experiments (see for instance the discussion in section II of [4]). The species dependent toroidal velocity gradient is then specified by:

$$\texttt{velocity\_toroidal\_gradient\_norm} = u'_{sN} = -\frac{L_{\text{ref}}^2}{v_{\text{thref}}}\frac{\partial\omega_{\varphi,s}}{\partial r},$$

that is positive for peaked profiles of a flow in the direction of $\nabla\varphi$.

Note that in the strict application of the local limit, i.e. for $\omega_{\varphi,s} = \omega_\Phi$, one has:

$$\gamma_{E_N} = -\frac{1}{2\pi L_{\text{ref}}B_{\text{ref}}}\frac{\partial\Psi}{\partial r}u'_{sN} = -\frac{RB_p}{L_{\text{ref}}B_{\text{ref}}}u'_{sN}$$

4.1.10 Plasma beta

The strength of the electromagnetic effects depends on the ratio of the plasma pressure to the magnetic energy and is specified by the dimensionless ratio:

$$\texttt{beta\_reference} = \beta_{eN} = 2\mu_0\frac{n_{\text{ref}}T_{\text{ref}}}{B_{\text{ref}}^2} \tag{4.1}$$

The plasma beta entering the Ampère's law is obtained from the reference value above combined with the species parameters (normalised density and temperature). When $\beta_{eN} = 0$, the run is electrostatic.

4.1.11 Debye length

The Debye length

$$\texttt{debye\_length\_reference} = \lambda_D = \sqrt{\frac{\epsilon_0 T_{\text{ref}}}{n_{\text{ref}}q_{\text{ref}}^2}} \tag{4.2}$$

enters the linearized quasi-neutrality equation. When neglected, this term is set to zero. In practice, it starts to matter for small scale ETG modes.

4.2 Magnetic equilibrium

The magnetic equilibrium in the vicinity of the flux surface of interest is specified by the parameters described in this section, given at $r = r_0$.

4.2.1 Radial position

$$\texttt{r\_minor\_norm} = r_N = \frac{r_0}{L_{\text{ref}}}$$

4.2.2 Toroidal field direction

$$\texttt{b\_field\_tor\_sign} = s_b = \text{sign}[\mathbf{B} \cdot \nabla\varphi]$$

4.2.3 Toroidal current direction

$$\texttt{ip\_sign} = s_j = \text{sign}[\mathbf{j} \cdot \nabla\varphi]$$

with j the plasma current density. For the conventions adopted in this document, positive plasma current implies positive poloidal magnetic field.

4.2.4 Safety factor

$$\texttt{q} = q = \frac{1}{2\pi} \int_0^{2\pi} \frac{\mathbf{B} \cdot \nabla\varphi}{\mathbf{B} \cdot \nabla\theta} \, d\theta$$

Note that q can be positive or negative, its sign depends on the sign of the toroidal plasma current and magnetic field:

$$q = s_b s_j |q|$$

4.2.5 Magnetic shear

$$\texttt{magnetic\_shear\_r\_minor} = \hat{s} = \frac{r}{q} \frac{\partial q}{\partial r}$$

4.2.6 Pressure gradient

$$\texttt{pressure\_gradient\_norm} = p'_N = -\frac{2\mu_0 L_{\text{ref}}}{B_{\text{ref}}^2} \frac{\partial p}{\partial r}$$

with p the total plasma pressure (i.e. the pressure term entering the Grad-Shafranov equation). p'_N (often called β') is a quantity related to the magnetic equilibrium and does not need to be consistent with the gradients (L_{ref}/L_{n_s}, L_{ref}/L_{T_s}) specified for the kinetic species.

Note that the low β' approximation for the curvature drift, i.e. the approximation

$$\mathbf{b} \times (\mathbf{b} \cdot \nabla \mathbf{b}) = \frac{1}{2}\mathbf{b} \times \nabla r \frac{2\mu_0}{B^2} \frac{\partial p}{\partial r} + \frac{\mathbf{B} \times \nabla B}{B^2} \sim \frac{\mathbf{B} \times \nabla B}{B^2},$$

is inconsistent with the use of a finite pressure gradient (p'_N) for the equilibrium description. The low β' approximation is nevertheless sometimes used in combination with the neglect of $B_\parallel$ fluctuations to take advantage of a cancellation at the MHD level [5]. This behaviour is controlled with the switch `inconsistent_curvature_drift` of the `model` table described in Sec. 4.6.2.

4.2.7 Plasma shape

A general description of local magnetic equilibria particularly convenient for gyrokinetic codes was introduced by J. Candy in [6]. It is used in the GKDB with a few minor modifications. The plasma shape is described by specifying the distance of the constant poloidal flux contours to the reference point (R_0, Z_0) normalised to L_{ref}:

$$a_N(r, \theta) = \frac{1}{L_{\text{ref}}} \sqrt{[R_{\Psi_0}(r, \theta) - R_0]^2 + [Z_{\Psi_0}(r, \theta) - Z_0]^2}$$

To allow regressions in the database the flux surface contours are parametrised as

$$a_N(r, \theta) = \sum_{n=0}^{N_{sh}} c_n \cos(n\theta) + s_n \sin(n\theta)$$

The specification of the local magnetic equilibrium then requires $4N_{sh} + 2$ terms, given at $r = r_0$, where N_{sh} is the degree of the expansion:

$$\texttt{shape\_coefficients\_c} = c_n$$
$$\texttt{shape\_coefficients\_s} = s_n$$
$$\texttt{dc\_dr\_minor\_norm} = \frac{\partial c_n}{\partial r_N}$$
$$\texttt{ds\_dr\_minor\_norm} = \frac{\partial s_n}{\partial r_N}$$

Typically $N_{sh} \leq 8$ is sufficient to capture most of the plasma shapes but higher values can be used when needed.

4.3 Modes

As almost every gyrokinetic code uses a different coordinate system, it is convenient to specify the Fourier modes in a coordinate free form.

To define this coordinate free form, let's first call, x and y, the radial and binormal coordinates used in gyrokinetic codes to describe the turbulence in the plane perpendicular to the magnetic field. The radial coordinate x is assumed to be a flux label (i.e. $\mathbf{B} \cdot \nabla x = 0$). In a spectral representation, perturbed quantities are then written:

$$f(x, y, \theta) = \sum_{k_x, k_y} \hat{f}(k_x, k_y, \theta) \exp[i k_x x + i k_y y] \tag{4.3}$$

where θ is used as the parallel coordinate. For a given mode, the perpendicular wave vector (in real space) is given by:

$$k_\perp^2(\theta) = k_x^2 g^{xx} + 2 k_x k_y g^{xy} + k_y^2 g^{yy} \tag{4.4}$$

with the code dependent metric elements given by $g^{ij} = \nabla i \cdot \nabla j$. All the metric information is on the right hand side of the equation above, the resulting $k_\perp$ does not depend on the specific coordinate choices made in gyrokinetic codes.

4.3.1 Radial wavevector

The normalised coordinate independent radial wavevector is defined as

$$\texttt{radial\_component\_norm} = k_{r*} \rho_{\text{ref}} = k_x \sqrt{g^{xx}(\theta = 0)} \rho_{\text{ref}} \tag{4.5}$$

4.3.2 Binormal wavevector

The normalised coordinate independent binormal wavevector is defined as

$$\texttt{binormal\_component\_norm} = k_{\theta*} \rho_{\text{ref}} = k_y \sqrt{g^{yy}(\theta = 0)} \rho_{\text{ref}} \tag{4.6}$$

An alternative convenient specification of the binormal wavevector is the effective poloidal mode number normalised to the ion Larmor radius $nq\rho_{\rm ref}/r_0$ [7]. This definition is also coordinate independent and related to a physical quantity. It will not be used here as there is no simple equivalent to specify the radial wave vector.

4.4 Number of poloidal turns

In the spectral representation of a flux-tube domain, the periodicity of the torus in the poloidal direction leads to the coupling of radial modes in the parallel direction:

$$\hat{f}(k_x, k_y, \theta - \pi) = \hat{f}(k_x + \Delta k_x, k_y, \theta + \pi)$$

with Δk_x depending on the magnetic shear.

A flux-tube extending over an odd number N_p of poloidal turns with 1 radial mode k_x is therefore equivalent to a flux-tube extending over 1 poloidal turn with N_p coupled radial modes $k_x + p\Delta k_x$ with p an integer varying from $-(N_p - 1)/2$ to $(N_p + 1)/2$. The number of poloidal turns (or coupled radial modes) is given by:

$$\texttt{poloidal\_turns} = N_p$$

This input is only used in the database for linear runs ($N_p = 1$ is enforced for non-linear runs). In practice, running with a sufficiently high number of poloidal turns (or coupled radial modes) is necessary to get a result independent of the boundary condition imposed at the end of the field line (when the number of poloidal turns increases, $k_\perp$ at the end of the field line increases and the perturbations are damped by finite Larmor radius effects).

4.5 Collisions

4.5.1 Plasma collisionality

To help capturing the variety of collisions implementation in gyrokinetic codes, the normalised collisionality is requested for each species couple a/b. It is defined as:

$$\texttt{collisionality\_norm} = \nu_N^{a/b} = \frac{L_{\rm ref}}{v_{\rm thref}} \frac{n_b Z_a^2 Z_b^2 e^4 \ln \Lambda^{a/b}}{4\pi\epsilon_0 m_a^2 v_{\rm tha}^3}$$

In addition, specific collisionality switches are described in Sec. 4.6.4. The exact definition of the Coulomb logarithm, $\ln \Lambda^{a/b}$, may vary from code to code, but this does not matter as it only appears within $\nu_N^{a/b}$.

4.6 Model

4.6.1 Linear or non-linear run

- Was it a linear or a non-linear run?

$$\texttt{non\_linear\_run} = \text{true / false}$$

- For linear runs, was it an initial value run or an eigenvalue run?

$$\texttt{initial\_value\_run} = \text{true / false}$$

- For non-linear runs, all the outputs are time averaged over the interval specified by

$$\texttt{time\_interval\_norm} = [t_{\rm start}; t_{\rm end}] \cdot \frac{v_{\rm thref}}{L_{\rm ref}}$$

13

4.6.2 Electromagnetic fluctuations

- Are the fluctuations of the parallel electromagnetic vector potential $A_\parallel$ retained (magnetic field flutter)?
$$\texttt{include\_a\_field\_parallel} = \text{true} \,/\, \text{false}$$

- Are the fluctuations of the perpendicular electromagnetic vector potential retained (magnetic field compression)?
$$\texttt{include\_b\_field\_parallel} = \text{true} \,/\, \text{false}$$

- Is the p'_N contribution to the curvature drift neglected?
$$\texttt{inconsistent\_curvature\_drift} = \text{true} \,/\, \text{false}$$

Note that $\texttt{inconsistent\_curvature\_drift} = \texttt{true}$ is only allowed with $\texttt{include\_b\_field\_parallel} = \texttt{false}$, see Sec. 4.2.6.

4.6.3 Rotation

- Are the centrifugal effects included?
$$\texttt{include\_centrifugal\_effects} = \text{true} \,/\, \text{false}$$

4.6.4 Collisions

- Pitch angle scattering only is retained (as opposed to pitch angle and energy scattering)
$$\texttt{collisions\_pitch\_only} = \text{true} \,/\, \text{false}$$

- Is momentum conservation ensured?
$$\texttt{collisions\_momentum\_conservation} = \text{true} \,/\, \text{false}$$

- Is energy conservation ensured?
$$\texttt{collisions\_energy\_conservation} = \text{true} \,/\, \text{false}$$

- Are finite Larmor radius effects retained in the collision treatment?
$$\texttt{collisions\_finite\_larmor\_radius} = \text{true} \,/\, \text{false}$$

Note that the implementation of collisions is highly code dependent and the list above does not give a complete characterisation of how collisions were treated in the run. However, this information can be retrieved from the specific code input file used for the run, which is also stored in the database.

4.7 Meta-data

4.7.1 Code specific data

For each point in the database, the following information is requested

- The name of the person (`provider`) submitting the entry to the database

- The name of the code (`name`)

- The version of the code (`version`) which should unambiguously allow to retrieve the source

- All the code specific inputs (with their code specific normalisation). This information will be stored in a key/value table (`parameters`) and used to rebuilt the input file when desired.

4.7.2 Comments

Informative comments can also be added (`comment` in the `ids_properties` table). For instance to indicate whether this entry is based on an experimental case or if it was used in a publication.

4.7.3 Tags

Different entries can be grouped together by giving them a common tag. This can be interesting when submitting entries from a parameter scan. Each tag has a name (`name`) and associated comments (`comments`).

Chapter 5

Outputs

5.1 Generalities

- For *linear* runs, all outputs are normalised to a dimensionless amplitude defined in the next section. The mode growth rate, frequency and convergence criterion (tolerance) are only filled for linear runs.

    - For *initial value* runs, there is only one eigenmode per wavevector (the most unstable mode) and the outputs are given at the last time step of the simulation (no time dependent information is stored)
    - For *eigenvalue* runs, there can be several eigenmodes per wavevector

- For *non-linear* runs, the fluxes, parallel mode structure and moments outputs are time averaged over the interval `time_interval_norm` specified in the `model` table.
  The `fluxes_integrated_norm` table, containing the fluxes summed over k_x and k_y, is only filled for non-linear runs.

5.2 Mode amplitude

In linear runs, unstable modes are exponentially growing in time and so are the associated fluxes. The exponentially growing outputs stored in the database are therefore normalised to a dimensionless mode amplitude defined as:

$$A_f(k_x, k_y) = \sqrt{\frac{1}{2\pi} \int \left[|\hat{\phi}_N(k_x, k_y, \theta)|^2 + |\hat{A}_{\parallel N}(k_x, k_y, \theta)|^2 + |\hat{B}_{\parallel N}(k_x, k_y, \theta)|^2 \right] \mathrm{d}\theta} \qquad (5.1)$$

with the Fourier components of the electrostatic potential and vector potential normalised as follows:

$$\hat{\phi}_N = \frac{1}{\rho_*} \frac{q_{\mathrm{ref}}}{T_{\mathrm{ref}}} \hat{\phi} \qquad \hat{A}_{\parallel N} = \frac{1}{\rho_*^2} \frac{1}{L_{\mathrm{ref}} B_{\mathrm{ref}}} \hat{A}_{\parallel} \qquad \hat{B}_{\parallel N} = \frac{1}{\rho_*} \frac{1}{B_{\mathrm{ref}}} \hat{B}_{\parallel} \qquad (5.2)$$

where $\rho_* = \rho_{\mathrm{ref}}/L_{\mathrm{ref}}$. The integral over θ is performed over the full length of the flux-tube (it is equivalent to an integral over one poloidal turn of the sum of all connected k_x modes).
The value of the mode amplitude in a linear run has little meaning by itself and is not stored in the database.
For non-linear runs, the dimensionless mode amplitude is taken to be

$$A_f(k_x, k_y) = 1$$

5.3 Mode growth rate and frequency (linear runs only)

The normalised mode growth rate γ and frequency ω_r are defined as:

$$\texttt{growth\_rate\_norm} = \gamma_N(k_x, k_y) = \gamma(k_x, k_y)\frac{L_{\text{ref}}}{v_{\text{thref}}}$$

$$\texttt{frequency\_norm} = \omega_{rN}(k_x, k_y) = \omega_r(k_x, k_y)\frac{L_{\text{ref}}}{v_{\text{thref}}}$$

By convention, unstable modes have a positive growth rate and modes propagating in the ion diamagnetic drift direction have a positive frequency (and therefore a negative frequency when they are propagating in the electron diamagnetic drift direction).

For initial value runs, the following (post-processing) method is used to determine the tolerance on the run convergence:

$$\texttt{growth\_rate\_tolerance} = \gamma_{\text{tol}} = \frac{1}{|\gamma_f|}\sqrt{\frac{1}{\Delta t}\int_{t_f-\Delta t}^{t_f}[\gamma(t) - \gamma_f]^2\,\mathrm{d}t}$$

where t_f and γ_f are the time and growth rate at the end of the simulation, respectively, $\Delta t = 3/(0.01 + |\gamma_f|)$ and

$$\gamma(t) = \frac{1}{\delta t}[\ln A_f(t) - \ln A_f(t - \delta t)]$$

with δt depending on the code setup but in any case several times smaller than Δt. Note that any exponentially growing quantity can be used in place of A_f to compute the time dependent growth rate. The tolerance on the growth rate still needs to be defined in a code independent way when an eigenvalue solver is used (input welcome!).

5.4 Fluxes

5.4.1 Definition

For each species, the flux-surface averaged contravariant radial component of the particle flux, energy flux and toroidal angular momentum flux, computed in particle phase space, are given by:

$$\Gamma_s = \left\langle \int \text{Re}\left[f_s^{gc}\right]\text{Re}\left[\mathbf{v_E} + \mathbf{v_{B_\perp}} + \mathbf{v}_{\nabla B_\parallel}\right] \cdot \nabla r\,\mathrm{d}\mathbf{v} \right\rangle \tag{5.3}$$

$$\Pi_s^\parallel = \left\langle \int s_b m_s R\frac{|B_t|}{B}v_\parallel \text{Re}\left[f_s^{gc}\right]\text{Re}\left[\mathbf{v_E} + \mathbf{v_{B_\perp}} + \mathbf{v}_{\nabla B_\parallel}\right] \cdot \nabla r\,\mathrm{d}\mathbf{v} \right\rangle \tag{5.4}$$

$$Q_s = \left\langle \int \frac{1}{2}m_s v^2 \text{Re}\left[f_s^{gc}\right]\text{Re}\left[\mathbf{v_E} + \mathbf{v_{B_\perp}} + \mathbf{v}_{\nabla B_\parallel}\right] \cdot \nabla r\,\mathrm{d}\mathbf{v} \right\rangle \tag{5.5}$$

where f_s^{gc} is the guiding center perturbed distribution function of species s (see Sec. 7.2.1 for the relationship with the gyro-center distribution function f_s). The three terms in the square brackets are the electrostatic, magnetic flutter and magnetic compression drifts:

$$\mathbf{v_E} = \frac{\mathbf{b} \times \nabla \langle\phi\rangle_{\text{gy}}}{B} \qquad \mathbf{v_{B_\perp}} = -v_\parallel\frac{\mathbf{b} \times \nabla \langle A_\parallel\rangle_{\text{gy}}}{B} \qquad \mathbf{v}_{\nabla B_\parallel} = \frac{\mu}{Z_s e}\frac{\mathbf{b} \times \nabla \langle B_\parallel\rangle_{\text{gy}}}{B} \tag{5.6}$$

with $\langle\phi\rangle_{\text{gy}}$, $\langle A_\parallel\rangle_{\text{gy}}$ and $\langle B_\parallel\rangle_{\text{gy}}$, the gyro-averaged perturbed electrostatic potential, parallel vector potential and parallel magnetic field, respectively.

The fluxes are positive when outward (for a transported quantity that is positive) and are given in the Laboratory frame. The relationship between fluxes expressed in the Laboratory frame and in the rotating frame of angular frequency ω_Φ is given in Sec. 7.1

Note that the momentum flux in the expression above only includes the toroidal projection of the parallel momentum. The toroidal projection of the perpendicular momentum also contributes to the total momentum flux, see e.g. [8]. This contribution is not included here but could be added in the future.

5.4.2   Spectral representation

Noting that

$$\left\langle \mathrm{Re}\left[A\right]\mathrm{Re}\left[\frac{\partial B}{\partial y}\right]\right\rangle = \sum_{k_x,k_y}\left\langle k_y\mathrm{Im}\left[\hat{A}(k_x,k_y,\theta)\hat{B}^\dagger(k_x,k_y,\theta)\right]\right\rangle$$

where A and B stand for any of the fluctuating fields, the fluxes can be expressed as

$$\Gamma_s = \sum_{k_x,ky}\Gamma_s(k_x,k_y) = \sum_{k_x,k_y>0}\left\langle k_y\mathcal{E}^{ry}\mathrm{Im}\left[\int J_0(k_\perp\rho_s)\hat{f}_s^{gc}\left[\hat{\phi}^\dagger - v_\|\hat{A}_\|^\dagger + \frac{\mu}{Z_se}\hat{B}_\|^\dagger\right]\mathrm{d}\mathbf{v}^*\right]\right\rangle$$

$$\Pi_s^\| = \sum_{k_x,ky}\Pi_s(k_x,k_y) = \sum_{k_x,k_y>0}\left\langle k_y\mathcal{E}^{ry}\mathrm{Im}\left[\int s_bm_sR\frac{|B_t|}{B}v_\|J_0(k_\perp\rho_s)\hat{f}_s^{gc}\left[\hat{\phi}^\dagger - v_\|\hat{A}_\|^\dagger + \frac{\mu}{Z_se}\hat{B}_\|^\dagger\right]\mathrm{d}\mathbf{v}^*\right]\right\rangle$$

$$Q_s = \sum_{k_x,ky}\Gamma_s(k_x,k_y) = \sum_{k_x,k_y>0}\left\langle k_y\mathcal{E}^{ry}\mathrm{Im}\left[\int \frac{1}{2}m_sv^2J_0(k_\perp\rho_s)\hat{f}_s^{gc}\left[\hat{\phi}^\dagger - v_\|\hat{A}_\|^\dagger + \frac{\mu}{Z_se}\hat{B}_\|^\dagger\right]\mathrm{d}\mathbf{v}^*\right]\right\rangle$$

where

$$\mathcal{E}^{ry} = \nabla r\cdot\frac{\mathbf{b}\times\nabla y}{B}\qquad\text{and}\qquad \mathrm{d}\mathbf{v}^* = \frac{2\pi B}{m}\mathrm{d}v_\|\mathrm{d}\mu$$

The integral over the gyro-angle has been performed analytically, resulting in the Bessel function J_0.

5.4.3   Normalisation

The fluxes are then given for each Fourier mode, normalised to the corresponding mode amplitude (taken to be 1 for non-linear runs) and made dimensionless as follows:

$$\Gamma_{sN}(k_x,k_y) = \frac{1}{A_f^2}\frac{\Gamma_s(k_x,k_y)}{n_sv_{\mathrm{thref}}\rho_*^2} \tag{5.7}$$

$$\Pi_{sN}(k_x,k_y) = \frac{1}{A_f^2}\frac{\Pi_s^\|(k_x,k_y)}{n_sm_{\mathrm{ref}}L_{\mathrm{ref}}v_{\mathrm{thref}}^2\rho_*^2} \tag{5.8}$$

$$Q_{sN}(k_x,k_y) = \frac{1}{A_f^2}\frac{Q_s(k_x,k_y)}{n_sT_{\mathrm{ref}}v_{\mathrm{thref}}\rho_*^2} \tag{5.9}$$

The electrostatic, magnetic flutter and magnetic compression contributions are stored separately (e.g. $\Gamma_{sN} = \Gamma_{sN,\phi} + \Gamma_{sN,A_\|} + \Gamma_{sN,B_\|}$) for each flux. The fluxes are normalised with respect to $n_s(\theta = 0)$ rather than n_{ref} to allow for trace species with zero density.

$$\mathtt{particles\_phi\_potential} = \Gamma_{sN,\phi}$$
$$\mathtt{particles\_a\_field\_parallel} = \Gamma_{sN,A_\|}$$
$$\mathtt{particles\_b\_field\_parallel} = \Gamma_{sN,B_\|}$$
$$\mathtt{momentum\_tor\_parallel\_phi\_potential} = \Pi_{sN,\phi}^\|$$
$$\mathtt{momentum\_tor\_parallel\_a\_field\_parallel} = \Pi_{sN,A_\|}^\|$$
$$\mathtt{momentum\_tor\_parallel\_b\_field\_parallel} = \Pi_{sN,B_\|}^\|$$
$$\mathtt{energy\_phi\_potential} = Q_{sN,\phi}$$
$$\mathtt{energy\_a\_field\_parallel} = Q_{sN,A_\|}$$
$$\mathtt{energy\_b\_field\_parallel} = Q_{sN,B_\|}$$

5.4.4 Total fluxes (non-linear runs only)

For non-linear runs, the total fluxes, defined as the sum of the fluxes over all the wavevectors, are also stored in the database:

$$\Gamma_{sN}^{\text{tot}} \quad = \sum_{k_x,k_y>0} 2\Gamma_{sN}(k_x,k_y) \tag{5.10}$$

$$\Pi_{sN}^{\text{tot}} \quad = \sum_{k_x,k_y>0} 2\Pi_{sN}^{\parallel}(k_x,k_y) \tag{5.11}$$

$$Q_{sN}^{\text{tot}} \quad = \sum_{k_x,k_y>0} 2Q_{sN}(k_x,k_y) \tag{5.12}$$

The total fluxes have the same names as the fluxes per wavevector but are stored in the table `fluxes_integrated_norm`.

5.5 Parallel mode structure

5.5.1 Parallel grid

The variation of the mode amplitude and phase in the parallel direction is given as a function of the poloidal angle θ defined previously. Note that the poloidal angle grid does not need to be uniform but has to be increasing.

$$\texttt{poloidal\_angle} = \theta$$

5.5.2 Perturbed electrostatic potential

$$\phi_{Nf}(\theta) = \frac{\hat{\phi}_N(k_x,k_y,\theta)}{A_f(k_x,k_y)}e^{i\alpha}$$

The phase factor α is chosen so that the imaginary part of ϕ_{Nf} is zero at $\theta = 0$ which makes comparisons of the mode structure between different runs easier. When $|\phi_{Nf}(\theta=0)| = 0$, α is taken to be zero. All the parallel outputs are rotated in the complex plane using the same value of α.

$$\texttt{phi\_potential\_perturbed\_norm\_real} = \text{Re}\left[\phi_{Nf}(\theta)\right]$$
$$\texttt{phi\_potential\_perturbed\_norm\_imaginary} = \text{Im}\left[\phi_{Nf}(\theta)\right]$$

5.5.3 Perturbed parallel vector potential (magnetic field flutter)

$$A_{\parallel Nf}(\theta) = \frac{\hat{A}_{\parallel N}(k_x,k_y,\theta)}{A_f(k_x,k_y)}e^{i\alpha}$$

$$\texttt{a\_field\_parallel\_perturbed\_norm\_real} = \text{Re}\left[A_{\parallel Nf}(\theta)\right]$$
$$\texttt{a\_field\_parallel\_perturbed\_norm\_imaginary} = \text{Im}\left[A_{\parallel Nf}(\theta)\right]$$

5.5.4 Perturbed parallel magnetic field (magnetic field compression)

$$B_{\parallel Nf}(\theta) = \frac{\hat{B}_{\parallel N}(k_x,k_y,\theta)}{A_f(k_x,k_y)}e^{i\alpha}$$

$$\texttt{b\_field\_parallel\_perturbed\_norm\_real} = \text{Re}\left[B_{\parallel Nf}(\theta)\right]$$
$$\texttt{b\_field\_parallel\_perturbed\_norm\_imaginary} = \text{Im}\left[B_{\parallel Nf}(\theta)\right]$$

5.5.5 Moments of the distribution function

Moments of the gyro-center distribution function, expressed in the Laboratory frame, can also be stored in the database. The moments are given as a function of the poloidal angle θ for each species and Fourier mode:

$$\delta n_s(\theta, k_x, k_y) = \int \hat{f}_s(\theta, k_x, k_y) \, \mathrm{d}\mathbf{v}^* \qquad \delta n_s^{J_0}(\theta, k_x, k_y) = \int J_0(k_\perp \rho_s) \hat{f}_s(\theta, k_x, k_y) \, \mathrm{d}\mathbf{v}^*$$

$$\delta v_{\|s}(\theta, k_x, k_y) = \int v_\| \hat{f}_s(\theta, k_x, k_y) \, \mathrm{d}\mathbf{v}^* \qquad \delta v_{\|s}^{J_0}(\theta, k_x, k_y) = \int v_\| J_0(k_\perp \rho_s) \hat{f}_s(\theta, k_x, k_y) \, \mathrm{d}\mathbf{v}^*$$

$$\delta T_{\perp s}(\theta, k_x, k_y) = \int \frac{1}{2} m_s v_\perp^2 \hat{f}_s(\theta, k_x, k_y) \, \mathrm{d}\mathbf{v}^* \qquad \delta T_{\perp s}^{J_0}(\theta, k_x, k_y) = \int \frac{1}{2} m_s v_\perp^2 J_0(k_\perp \rho_s) \hat{f}_s(\theta, k_x, k_y) \, \mathrm{d}\mathbf{v}^*$$

$$\delta T_{\|s}(\theta, k_x, k_y) = \int \frac{1}{2} m_s v_\|^2 \hat{f}_s(\theta, k_x, k_y) \, \mathrm{d}\mathbf{v}^* \qquad \delta T_{\|s}^{J_0}(\theta, k_x, k_y) = \int \frac{1}{2} m_s v_\|^2 J_0(k_\perp \rho_s) \hat{f}_s(\theta, k_x, k_y) \, \mathrm{d}\mathbf{v}^*$$

with J_0 the Bessel function. The normalisation of the moments is given by:

$$\delta n_{sN} = \frac{\delta n_s}{n_s A_f \rho_*} \mathrm{e}^{i\alpha} \qquad\qquad \delta n_{sN}^{J_0} = \frac{\delta n_s^{J_0}}{n_s A_f \rho_*} \mathrm{e}^{i\alpha}$$

$$\delta v_{\|sN} = \frac{\delta v_{\|s}}{n_s v_{\mathrm{thref}} A_f \rho_*} \mathrm{e}^{i\alpha} \qquad\qquad \delta v_{\|sN}^{J_0} = \frac{\delta v_{\|s}^{J_0}}{n_s v_{\mathrm{thref}} A_f \rho_*} \mathrm{e}^{i\alpha}$$

$$\delta T_{\perp sN} = \frac{\delta T_{\perp s}}{n_s T_{\mathrm{ref}} A_f \rho_*} \mathrm{e}^{i\alpha} \qquad\qquad \delta T_{\perp sN}^{J_0} = \frac{\delta T_{\perp s}^{J_0}}{n_s T_{\mathrm{ref}} A_f \rho_*} \mathrm{e}^{i\alpha}$$

$$\delta T_{\|sN} = \frac{\delta T_{\|s}}{n_s T_{\mathrm{ref}} A_f \rho_*} \mathrm{e}^{i\alpha} \qquad\qquad \delta T_{\|sN}^{J_0} = \frac{\delta T_{\|s}^{J_0}}{n_s T_{\mathrm{ref}} A_f \rho_*} \mathrm{e}^{i\alpha}$$

As for the fluxes, the normalisation is with respect to $n_s(\theta = 0)$ to allow for trace species with zero densities.

Chapter 6

Derived quantities

The derived quantities are computed internally when an entry is submitted to the GKDB and stored in the database. They can then be used for queries.

6.1 Relative fields weight

The ratio of each field to the total mode amplitude is stored:

$$\texttt{phi\_potential\_perturbed\_weight} = A_\phi = \sqrt{\frac{1}{2\pi} \int |\phi_{Nf}(\theta)|^2 \, \mathrm{d}\theta}$$

$$\texttt{a\_field\_parallel\_perturbed\_weight} = A_{A_\parallel} = \sqrt{\frac{1}{2\pi} \int |A_{\parallel Nf}(\theta)|^2 \, \mathrm{d}\theta}$$

$$\texttt{b\_field\_parallel\_perturbed\_weight} = A_{B_\parallel} = \sqrt{\frac{1}{2\pi} \int |B_{\parallel Nf}(\theta)|^2 \, \mathrm{d}\theta}$$

6.2 Fields parity

The field parity is computed as follows:

$$\texttt{phi\_potential\_perturbed\_parity} = \pi_\phi = \frac{\left| \int \phi_{Nf}(\theta) \, \mathrm{d}\theta \right|}{\int |\phi_{Nf}(\theta)| \, \mathrm{d}\theta}$$

$$\texttt{a\_field\_parallel\_perturbed\_parity} = \pi_{A_\parallel} = \frac{\left| \int A_{\parallel Nf}(\theta) \, \mathrm{d}\theta \right|}{\int |A_{\parallel Nf}(\theta)| \, \mathrm{d}\theta}$$

$$\texttt{b\_field\_parallel\_perturbed\_parity} = \pi_{B_\parallel} = \frac{\left| \int B_{\parallel Nf}(\theta) \, \mathrm{d}\theta \right|}{\int |B_{\parallel Nf}(\theta)| \, \mathrm{d}\theta}$$

6.3 Conventional shape parameters

The flux surface elongation κ, top triangularity δ_{top} and bottom triangularity δ_{bot} are computed as follows:

$$\texttt{elongation} = \kappa = \frac{Z_{\max} - Z_{\min}}{R_{\max} - R_{\min}}$$

$$\texttt{triangularity\_upper} = \delta^{\mathrm{top}} = \frac{R_{\Psi_0}(Z_{\max}) - R_0}{r_0}$$

$$\texttt{triangularity\_lower} = \delta^{\mathrm{bot}} = \frac{R_{\Psi_0}(Z_{\min}) - R_0}{r_0}$$

with $R_{\min} = \min[R_{\Psi_0}]$, $R_{\max} = \max[R_{\Psi_0}]$, $Z_{\min} = \min[Z_{\Psi_0}]$ and $Z_{\max} = \max[Z_{\Psi_0}]$.

6.4 Global species parameters

6.4.1 Effective charge

To have a fast and simple way to query on the plasma composition, the effective charge is computed:

$$\texttt{zeff} = Z_{\text{eff}} = \sum_{\text{ions}} n_{sN} Z_{sN}^2$$

6.4.2 Sum over duplicated species

To make query on entries with duplicate species more convenient, a duplicate species index is built that allow to query directly on:

$$n_{sN} = \sum_{s_i} n_{s_i N}, \qquad \frac{L_{\text{ref}}}{L_{n_s}} = \frac{1}{n_{sN}} \sum_{s_i} n_{s_i N} \frac{L_{\text{ref}}}{L_{n_{s_i}}}, \qquad \frac{L_{\text{ref}}}{L_{T_s}} = \frac{1}{n_{sN}} \sum_{s_i} n_{s_i N} \frac{L_{\text{ref}}}{L_{T_{s_i}}}$$

with s_i the duplicated species entries for species s, identified by their common charge, mass and temperature.

Chapter 7

Transformation of database outputs

7.1 Laboratory frame versus rotating frame

To describe inertial effects associated with the background rotation, several gyrokinetic codes (e.g. GKW, GENE, GS2) solve the gyro-kinetic equation in the frame rotating as a rigid body with the angular frequency ω_Φ. The fluxes and moments stored in the database are expressed in the Laboratory frame. Their link with the fluxes and moments expressed in the rotating frame is documented below.

7.1.1 Fluxes

The Laboratory frame fluxes are related to the rotating frame fluxes as follows:

$$\Gamma_s^{\mathrm{L}} = \Gamma_s^{\mathrm{co}} \tag{7.1}$$

$$\Pi_s^{\|\mathrm{L}} = \Pi_s^{\|\mathrm{L}} + \left\langle \int m_s \omega_\Phi \left(\frac{RB_t}{B} \right)^2 \mathrm{Re}\,[f_s^{\mathrm{co}}]\,\mathrm{Re}\,[\mathbf{v}_\chi \cdot \nabla r]\,\mathrm{d}\mathbf{v} \right\rangle \tag{7.2}$$

$$Q_s^{\mathrm{L}} = Q_s^{\mathrm{co}} + \omega_\Phi \Pi_s^{\|\mathrm{L}} + \left\langle \int \frac{1}{2} m_s (R\omega_\Phi)^2 \mathrm{Re}\,[f_s^{\mathrm{co}}]\,\mathrm{Re}\,[\mathbf{v}_\chi \cdot \nabla r]\,\mathrm{d}\mathbf{v} \right\rangle \tag{7.3}$$

with $\mathbf{v}_\chi = \mathbf{v_E} + \mathbf{v_{B\perp}} + \mathbf{v}_{\nabla B_\|}$ and all the expressions in the right hand sides evaluated in the rotating frame.

7.1.2 Moments

Similarly, the moments of the distribution function in the Laboratory frame can be expressed as a function of their counterpart in the rotating frame:

$$\delta n_s^{\mathrm{L}} = \delta n_s^{\mathrm{co}}$$

$$\delta v_{\|s}^{\mathrm{L}} = \delta v_{\|s}^{\mathrm{co}} + s_b R\omega_\Phi \frac{|B_t|}{B} \delta n_s^{\mathrm{co}}$$

$$\delta T_{\perp s}^{\mathrm{L}} = \delta T_{\perp s}^{\mathrm{co}} + m_s \left[R\omega_\Phi \frac{B_p}{B} \right]^2 \delta n_s^{\mathrm{co}}$$

$$\delta T_{\|s}^{\mathrm{L}} = \delta T_{\|s}^{\mathrm{co}} + s_b m_s R\omega_\Phi \frac{|B_t|}{B} \delta v_{\|s}^{\mathrm{co}} + m_s \left[R\omega_\Phi \frac{B_t}{B} \right]^2 \delta n_s^{\mathrm{co}}$$

7.2 Computing the fluxes from the gyro-averaged moments

Most of the fluxes can be computed from the gyro-averaged moments stored in the database. This calculation is described below.

7.2.1 Relationship between guiding-center and gyro-center distribution functions

The guiding center distribution function f_s^{gc} is related to the gyro-center distribution function f_s by:

$$f_s^{gc} = f_s - \frac{F_{Ms}}{T_s}\left[Z_s e[\phi - \langle\phi\rangle_{\text{gy}}] + \mu\left\langle B_\parallel\right\rangle_{\text{gy}}\right]$$

where F_{Ms} is the Maxwellian background of species s.

7.2.2 Polarisation and magnetisation effects

The fluxes computed in particle phase space (see Sec. 5.4) can therefore be written as

$$\Gamma_s = \Gamma_s^{\text{gy}} + \Gamma_s^{\text{pol}} + \Gamma_s^{\text{mag}}$$
$$\Pi_s^\parallel = \Pi_s^{\parallel\text{gy}} + \Pi_s^{\parallel\text{pol}} + \Pi_s^{\parallel\text{mag}}$$
$$Q_s = Q_s^{\text{gy}} + Q_s^{\text{pol}} + Q_s^{\text{mag}}$$

where the fluxes with the 'gy' superscript are computed with the gyro-center distribution function f_s instead of the guiding center distribution function f_s^{gc}, and where the polarisation and magnetisation components are defined as:

$$\Gamma_s^{\text{pol}}(k_x, k_y) = -\left\langle k_y\mathcal{E}^{ry}\text{Im}\left[\int J_0(1-J_0)F_{Ms}\frac{Z_s e}{T_s}\hat{\phi}\left[-v_\parallel\hat{A}_\parallel^\dagger + \frac{\mu}{Z_s e}\hat{B}_\parallel^\dagger\right]\,\mathrm{d}\mathbf{v}^*\right]\right\rangle$$

$$\Gamma_s^{\text{mag}}(k_x, k_y) = -\left\langle k_y\mathcal{E}^{ry}\text{Im}\left[\int \mu J_0^2 F_{Ms}\frac{1}{T_s}\hat{B}_\parallel\left[\hat{\phi}^\dagger - v_\parallel\hat{A}_\parallel^\dagger\right]\,\mathrm{d}\mathbf{v}^*\right]\right\rangle$$

$$\Pi_s^{\parallel\text{pol}}(k_x, k_y) = -\left\langle k_y\mathcal{E}^{ry}\text{Im}\left[\int s_b m_s R\frac{|B_t|}{B}v_\parallel J_0(1-J_0)F_{Ms}\frac{Z_s e}{T_s}\hat{\phi}\left[-v_\parallel\hat{A}_\parallel^\dagger + \frac{\mu}{Z_s e}\hat{B}_\parallel^\dagger\right]\,\mathrm{d}\mathbf{v}^*\right]\right\rangle$$

$$\Pi_s^{\parallel\text{mag}}(k_x, k_y) = -\left\langle k_y\mathcal{E}^{ry}\text{Im}\left[\int s_b m_s R\frac{|B_t|}{B}v_\parallel\mu J_0^2 F_{Ms}\frac{1}{T_s}\hat{B}_\parallel\left[\hat{\phi}^\dagger - v_\parallel\hat{A}_\parallel^\dagger\right]\,\mathrm{d}\mathbf{v}^*\right]\right\rangle$$

$$Q_s^{\text{pol}}(k_x, k_y) = -\left\langle k_y\mathcal{E}^{ry}\text{Im}\left[\int \frac{1}{2}m_s v^2 J_0(1-J_0)F_{Ms}\frac{Z_s e}{T_s}\hat{\phi}\left[-v_\parallel\hat{A}_\parallel^\dagger + \frac{\mu}{Z_s e}\hat{B}_\parallel^\dagger\right]\,\mathrm{d}\mathbf{v}^*\right]\right\rangle$$

$$Q_s^{\text{mag}}(k_x, k_y) = -\left\langle k_y\mathcal{E}^{ry}\text{Im}\left[\int \frac{1}{2}m_s v^2 \mu J_0^2 F_{Ms}\frac{1}{T_s}\hat{B}_\parallel\left[\hat{\phi}^\dagger - v_\parallel\hat{A}_\parallel^\dagger\right]\,\mathrm{d}\mathbf{v}^*\right]\right\rangle$$

7.2.3 Fluxes and gyro-averaged moments

The next step is to express the fluxes of gyro-centers as a function of the gyro-averaged moments stored in the database:

$$\Gamma_s^{gy}(k_x, k_y) = \left\langle k_y\mathcal{E}^{ry}\left[\text{Im}\left[\delta n_s^{J_0}\hat{\phi}^\dagger\right] - \text{Im}\left[\delta v_{\parallel s}^{J_0}\hat{A}_\parallel^\dagger\right] + \frac{2}{Z_s eB}\text{Im}\left[\delta T_{\perp s}^{J_0}\hat{B}_\parallel^\dagger\right]\right]\right\rangle$$

$$\Pi_s^{\parallel\text{gy}}(k_x, k_y) = \left\langle k_y\mathcal{E}^{ry}s_b m_s R\frac{|B_t|}{B}\left[\text{Im}\left[\delta v_{\parallel s}^{J_0}\hat{\phi}^\dagger\right] - \frac{2}{m_s}\text{Im}\left[\delta T_{\parallel s}^{J_0}\hat{A}_\parallel^\dagger\right] + \frac{m_s}{Z_s eB}\text{Im}\left[\delta m_s^{J_0}(v_\parallel v_\perp^2)\hat{B}_\parallel^\dagger\right]\right]\right\rangle$$

$$Q_s^{gy}(k_x, k_y) = \left\langle k_y\mathcal{E}^{ry}\left[\text{Im}\left[(\delta T_{\parallel s}^{J_0} + \delta T_{\perp s}^{J_0})\hat{\phi}^\dagger\right] - \text{Im}\left[\delta m_s^{J_0}(\frac{1}{2}m_s v_\parallel v^2)\hat{A}_\parallel^\dagger\right] + \frac{m_s}{Z_s eB}\text{Im}\left[\delta m_s^{J_0}(\frac{1}{2}m_s v_\perp^2 v^2)\hat{B}_\parallel^\dagger\right]\right]\right\rangle$$

where the

$$\delta m_s^{J_0}(x) = \int x J_0(k_\perp\rho_s)\hat{f}_s(\theta, k_x, k_y)\,\mathrm{d}\mathbf{v}^*$$

are higher order moments not stored in the database.

7.2.4 Metric coefficients

Compute $\mathcal{E}^{ry}$ and the flux surface average from the data in the `flux_surface` table.

Chapter 8

Entry submission procedure

Explain that the entries are submitted to the db with a json file and point at the relevant documentation on the wikipages of the git repository.

8.1 Reference cases

8.2 Checks

8.2.1 Requirements

- A species is identified by its charge, mass and temperature. The species with a negative charge is the electron species.

- The charge, mass, temperature and density of the electron species are:

$$Z_{eN} = -1, \qquad m_{sN} = 2.7237 \times 10^{-4} \qquad T_{eN} = 1 \qquad n_{eN} = 1 \qquad (8.1)$$

- The species density and their gradients must satisfy quasineutrality:

$$\sum_s Z_{sN} n_{sN} = 0 \qquad \sum_s Z_{sN} \frac{n_{sN}}{L_{n_s}} = 0 \qquad (8.2)$$

- If at least one species has its Mach number $M_s = u_N \sqrt{m_{sN}/T_{sN}} > 0.2$, centrifugal effects must be included

- If $\beta_{eN} > 0$, magnetic flutter has to be included: `include_a_field_parallel = true`

- If $\beta_{eN} > 0.5\%$, magnetic compression has to be included: `include_b_field_parallel = true` unless the β' contribution to the curvature drift is neglected, i.e. `inconsistent_curvature_drift = true`, see Sec. 4.2.6.

- The tolerance on the mode growth rate can not be more than 10%.

- For initial value runs, $N_{\text{modes}} = 1$.

- The poloidal angle array must range from $-N_p\pi$ to $N_p\pi$, with N_p the number of poloidal turns.

- The arrays containing the parallel structure of the fields are of size $N_{\text{pol grid}} \times N_{\text{modes}}$ with $N_{\text{pol grid}}$ the length of the poloidal angle array.

- The fields have been rotated in the complex plane so that $\text{Im}\,[\phi_{Nf}(\theta = 0)] = 0$. Note that the ϕ_{Nf} array does not necessarily have a point at $\theta = 0$. In that case, the condition above is checked by interpolating ϕ_{Nf} at $\theta = 0$.

- The array containing the fluxes are of size $N_{\text{species}} \times N_{\text{modes}}$, i.e. one flux value is given per species and per mode (there may be several mode per wavevector when an eigenvalue solver is used).

8.2.2 Mandatory fields

All fields are mandatory, except the parallel structure of moments of the distribution function and, of course, the internally derived fields.

8.2.3 Consistency checks

- The r_N input should be consistent with the flux surface shape description $\{c_n, s_n\}$

$$r_N = \frac{1}{2} \left[\max[a_N(\theta)\cos\theta] - \min[a_N(\theta)\sin\theta] \right]$$

8.2.4 Sanity checks

- If the amplitude of a field ($|\phi_{Nf}|$, $|A_{\|Nf}|$ or $|B_{\|Nf}|$) at the end of a field line is more than 5% of its maximum, the number of poloidal turns should be increased.

- An attempt to detect runs that were numerically unstable in the parallel direction is made by testing that:

8.3 Append wave vectors to an entry

On user request. Automatically check that the point is identical.

Chapter 9

Test cases

9.1   Test 1

A simple electrostatic test case close to the GA standard case with kinetic electrons.

Bibliography

[1] O. Sauter and S.Yu. Medvedev. *Comput. Phys. Comm.*, 184:293, 2013.

[2] F.L. Hinton and R.D. Hazeltine. *Rev. Mod. Phys.*, 48:239, 1976.

[3] S.P. Hirshman and D.J. Sigmar. *Nucl. Fusion*, 21:1079, 1981.

[4] Y. Camenen *et al. Phys. Plasmas*, 23:022507, 2016.

[5] R.E. Waltz and R.L. Miller. *Phys. Plasmas*, 6:4265, 1999.

[6] J. Candy. *Plasma Phys. Control. Fusion*, 51:105009, 2009.

[7] G. Merlo, O. Sauter, *et al. Phys. Plasmas*, 23:032104, 2016.

[8] B. Scott and J. Smirnov. *Phys. Plasmas*, 17:112302, 2010.